Informatics in Medicine Unlocked 25 (2021) 100706

Contents lists available at ScienceDirect

Informatics in Medicine Unlocked

journal homepage: www.elsevier.com/locate/imu

Physicochemical, spectral, molecular docking and ADMET studies of Bisphenol analogues; A computational approach

Monir Uzzaman [a,*], Md. Kamrul Hasan [b], Shafi Mahmud [c], Abu Yousuf [d], Saidul Islam [e], Mohammad Nasir Uddin [a], Ayan Barua [a]

[a] Faculty of Science, Department of Chemistry, University of Chittagong, Chittagong, 4331, Bangladesh
[b] Department of Theoretical and Computational Chemistry, University of Dhaka, Dhaka, 1000, Bangladesh
[c] Department of Genetic Engineering and Biotechnology, University of Rajshahi, Bangladesh
[d] Department of Applied Chemistry and Chemical Engineering, University of Chittagong, Chittagong, 4331, Bangladesh
[e] Department of Pharmacy, University of Chittagong, Chittagong, 4331, Bangladesh

ARTICLE INFO

Keywords:
Bisphenols
Endocrine disrupt
Molecular docking and dynamics simulation
ADMET

ABSTRACT

Bisphenols are widely used in polymer and packaging industries. But they are contaminating the environment and food chain by degradation, particularly affecting to the human endocrine system. Herein, we have investigated the physicochemical, spectral, biological and pharmacokinetic properties of some selected bisphenol analogues utilizing computer-aided drug design methods. Geometry optimization has been performed by employing density functional theory with B3LYP/6-311g++ (d, p) basis set. Geometrical, thermodynamical, molecular orbital and electrostatic potential studies have been calculated to investigate their physical and chemical behavior. Meanwhile, FT-IR, Raman and UV-Vis's spectra have been measured and compared with the experimental values. Molecular docking and dynamics simulation studies have been performed against human estrogen-related receptor protein to investigate their binding affinity, mode and interactions with the receptor. ADMET prediction has been performed to compare their absorption, distribution, metabolism and toxicity. Among the studied analogues, Bis AF has the highest free energy and Bis E has highest binding affinity. Meanwhile, Bis S shows the highest dipole moment and the chemical reactivity. Most of them have inhibitory property to the CYP2C9 and Bis S shows the carcinogenic property. Based on the comparative physicochemical, spectral, biological and ADMET calculation, this study can be helpful to understand more deeply about their biochemical impact on the environment and human being.

1. Introduction

Bisphenols (Bis) are widely used in polymer and packaging industries [1]. The core structure of bisphenol made by two hydroxyphenyl functional groups which are connected through a bridging carbon. The insertion of different functional groups at the phenolic ring and bridging carbon differentiates them into various analogues [2]. Bis A is used in the production of polycarbonate plastic and epoxy resins, containers, electronics and medical equipment's [3,4]. It degrades in several ways and produce some more toxic intermediates; meanwhile completely degraded products are relatively less toxic than that of Bis A [5–7]. It detected everywhere in the environment and human are exposed to this chemical via food, inhalation of household dust and dermal exposure [1,3,8]. Previous researches have confirmed the presence of Bis A in human urine, serum, breast milk, placental tissue, umbilical cord blood, fetal livers, follicular and amniotic fluid [3]. It is described as endocrine disruptor chemical (EDC), able to bind and activate the human estrogen receptor [9,10]. In particular, some crucial adverse effects on reproduction i.e., fertility, male sexual function, sperm quality, sex hormone concentration, breast cancer, miscarriage and premature delivery; development i.e., birth weight, male genital abnormalities, neurodevelopment and childhood asthma; metabolic diseases i.e., type-2 diabetes, hypertension, cardiovascular diseases; others effect i.e., inflammation, oxidative stress, immune function, epigenetics and gene expression [1,11–13]. It may breakdown the double stranded DNAs and interfere in normal human development [14]. Resulting, Canadian [4] and French government [15] banned the usages of products containing Bis A in 2010. Similarly, European Union in 2011 [4] and Food and Drug

* Corresponding author. Faculty of science, Department of Chemistry, University of Chittagong, Chittagong, 4331, Bangladesh.
E-mail address: monircu92@gmail.com (M. Uzzaman).

https://doi.org/10.1016/j.imu.2021.100706
Received 2 July 2021; Received in revised form 14 August 2021; Accepted 14 August 2021
Available online 18 August 2021

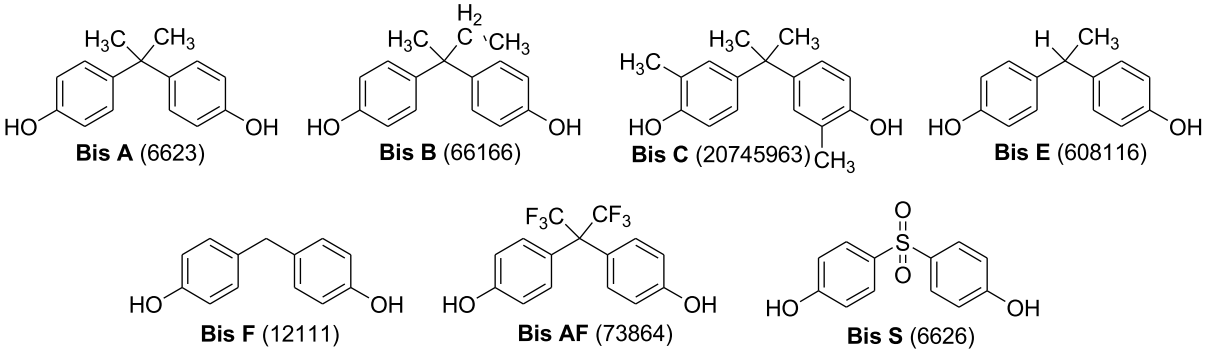

Fig. 1. Chemical structures of bisphenol analogues with PubChem ID.

Administration in 2012 [16] prohibited the use of Bis A in baby feeding bottles [17].

To overcome these difficulties, some other analogues such as; Bis B, Bis C, Bis E, Bis F, Bis AF, Bis S etc. have been introduced in the manufacturing of food contact materials [18]. Among these, Bis F has various applications, including food packaging, coating, oral prosthetic devices, dental sealants, lacquers and varnishes [19]. Bis AF is a cross-linker in optical fibers and fluor elastomers, a high-performance monomer in polyamides, polyesters and in waveguides and plastic optical fibers [20,21]. Bis S is an anti-corrosive agent in epoxy glues and a polymer reaction [22], as an additive in dyes and tanning agents [23]. Unfortunately, these analogues also have some toxic effects to the environment and human beings. Their endocrine disrupting effects, reproductive toxicity, neurotoxicity, cytotoxicity, genotoxicity and dioxin-like toxicity already reported by many researchers [4]. Bis S and Bis F are not safe alternative of Bis A; which is notified in several studies [24]. Some bisphenol analogues such as Bis B, Bis F, Bis AF and Bis S have almost similar or even more significant genotoxicity and estrogenic activity than Bis A [2,25]. Bis AF and Bis B show a higher estrogenic effect than Bis A [26]. Bis AF also causes the reduction of testosterone hormone in adult male rat [27]. These side effects suggest to awareness about the safety concern of bisphenol analogues and think deeply about their applications as replacement of Bis A. Previously, numerous researches have been reported about the synthesis, detection, removing, human exposure and toxicity of Bis A and some of its selected analogues, still gap of knowledge and research are required to this field.

Herein we have reported the thermodynamic, molecular orbital, electrostatic potential, geometrical, FT-IR, Raman, UV-Vis, molecular docking, dynamics simulation, non-bonding interactions and ADMET analysis of seven selected Bis analogues. To the best of our knowledge, we are the very first doing such investigations which containing all above-mentioned characteristics collectively. Definitely this study will help to understand the physical, chemical, spectral, biological and toxicological behaviors of mentioned analogues and to design relatively safe candidates.

2. Methods and materials

2.1. Geometry optimization details

The initial geometry of all analogues (Fig. 1) was collected from an online structure database PubChem. Geometry optimization and further calculation were carried out by utilizing Gaussian 09W Revision (D.01) [28] software. Density functional theory (DFT) along with Backe's (B) three-parameter hybrid model; Lee, Yang and Parr's (LYP) correlation functional under Pople's 6–311g++ (d, p) basis set was employed to calculate their physicochemical and spectral properties. Time dependent density functional theory (TD-DFT) has been incorporated to investigate the electronic excited states. Global chemical reactivity has been calculated by analyzing molecular orbital features using following equations;

$$\text{Gap}\quad(\Delta E) = [\varepsilon\text{LUMO} - \varepsilon\text{HOMO}];\ \eta = \frac{[\varepsilon\text{LUMO} - \varepsilon\text{HOMO}]}{2};\ S = \frac{1}{\eta}$$

$$\mu = \frac{[\varepsilon\text{LUMO} + \varepsilon\text{HOMO}]}{2};\ \chi = -\frac{[\varepsilon\text{LUMO} + \varepsilon\text{HOMO}]}{2};\ \omega = \frac{\mu^2}{2\eta}$$

2.2. Protein preparation, docking simulation, analysis and visualization

3D crystal structure of human estrogen-related receptor protein (2E2R), co-crystallized with Bis A ligand was retrieved from RCSB protein data bank (PDB) at 1.60 Å resolution in pdb format. Hetero atoms, water molecules and co-crystallized ligand were deleted to prepare the protein chain using PyMol (1.3), then subjected for energy minimization to remove the bad contacts of protein utilizing Swiss-PDB Viewer (4.1.0). Finally, docking simulation was performed using PyRx (0.8) software considering the protein as macromolecule and compounds as ligand by maintaining grid box size 56.39, 46.77 and 43.14 Å along X, Y, and Z directions respectively, where the whole protein was covered by grid box. Both the protein and docked structure were saved in pdb format to calculate the non-bonding interactions. Discovery Studio Visualizer was utilized to predict, analyze and visualize the interactions between ligand and amino acid residues of receptor protein.

2.3. Molecular dynamics simulation

The molecular dynamics simulation study was conducted in YASARA dynamics with the aid of the AMBER14 force field [29,30]. The docked complexes were initially cleaned and optimized, and hydrogen bond networks were oriented. The cubic simulation cell was created with TIP3P solvation model with periodic boundary conditions [31]. The physiological states of the simulation's cells were set as 310K, pH 7.4, and 0.9% NaCl. The energy minimizations of the simulations systems were done with the aid of the steepest gradient algorithms (5000 Cycles) by simulated annealing methods. The simulation time step was set as 2.0 fs. The long range electrostatic interactions were calculated by the Particle Mesh Ewalds algorithms by a cut off radius of 8.0 Å [32,33]. The simulation trajectories were saved after every 100 ps. By following the constant pressure and Berendsen thermostat, the simulations were run for 100 ns [34]. The simulation trajectories were utilized to calculate the root mean square deviations, the root mean square fluctuations, hydrogen bonds, solvent accessible surface area and radius of gyration [35–39].

2.4. ADMET prediction

Pharmacokinetic parameters are related to drug absorption, distribution, metabolism and toxicity were calculated utilizing online server AdmetSAR. Structure data files and simplified molecular-input line-

Table 1
Molecular formula (MF), molecular weight (MW), dipole moment (Debye) and energies (Hartree) of bisphenol analogues.

Name	MF	MW	Dipole moment	Internal energy	Enthalpy	Free energy
Bis A	$C_{15}H_{16}O_2$	228.286	0.920	−731.590	−731.589	−731.648
Bis B	$C_{16}H_{18}O_2$	242.313	0.872	−770.882	−770.881	−770.943
Bis C	$C_{17}H_{20}O_2$	256.340	1.932	−810.186	−810.185	−810.252
Bis E	$C_{14}H_{14}O_2$	214.260	2.545	−692.300	−692.299	−692.357
Bis F	$C_{13}H_{12}O_2$	200.233	2.356	−653.008	−653.007	−653.062
Bis AF	$C_{15}H_{10}F_6O_2$	336.229	4.752	−1327.266	−1327.265	−1327.333
Bis S	$C_{12}H_{10}O_4S$	250.270	5.571	−1162.342	−1162.341	−1162.400

Table 2
Energy (eV) of HOMO-LUMO, gap, hardness (η), softness (S), chemical potential (μ), electronegativity (χ) and electrophilicity (ω) of bisphenol analogues.

Name	ϵHOMO	ϵLUMO	Gap	η	S	μ	χ	ω
Bis A	−5.990	−0.625	5.365	2.683	0.186	−3.308	3.308	2.039
Bis B	−5.975	−0.616	5.359	2.679	0.186	−3.296	3.296	2.028
Bis C	−5.829	−0.456	5.373	2.686	0.186	−3.143	3.143	1.839
Bis E	−6.008	−0.623	5.385	2.693	0.186	−3.316	3.316	2.042
Bis F	−6.052	−0.698	5.354	2.677	0.187	−3.375	3.375	2.127
Bis AF	−6.621	−1.070	5.551	2.775	0.180	−3.846	3.846	2.665
Bis S	−6.766	−1.494	5.272	2.636	0.190	−4.130	4.130	3.235

entry system strings were utilized throughout the conversion procedure.

3. Result and discussion

3.1. Thermodynamic analysis

Thermochemical calculations help to predict the reaction kinetics and chemical stability of the reaction products. Mainly free energy and enthalpy are related to the absorption or release of energy in a chemical reaction and a molecule's chemical stability [40,41]. The free energy value is the key factor in study about the easy binding potential with the other compounds where both sign and magnitudes are bear unique characteristics of a compound. The negative sign reveals the spontaneous binding and the high value alludes to the more available bindings [42,43]. Here, the free energy and enthalpy values of all the compounds are negative (Table 1), which turns no external energy will be needed for bindings. The high electronegative molecules (fluorine and oxygen) present in Bis AF and Bis S show a high energy value than the other Bis analogues. The rest of the compounds show fewer binding interactions than Bis AF and Bis S. The improved thermodynamic properties of Bis AF and Bis S relative to the other Bisphenol analogues are indicated by higher energy values (internal and free energy) and enthalpy values with a negative sign. Here, the enthalpy values of Bis AF and Bis S are −1327.266 Hartree and −1162.342 Hartree respectively where that of Bis C is −810.186 Hartree, which is the third-highest value. On the other hand, Bis AF and Bis S are containing CF_3 and SO_2 functional groups in their chemical structures have relatively higher free energy values which are −1327.333 Hartree and −1162.400 Hartree.

The dipole moment value of a molecule is very significant to describe its electronic property, where a high dipole moment value of a molecule plays more intermolecular interactions. High dipole moment value reveals more polar nature [44–46]. From Table 1, Bis AF (4.762 Debye) and Bis S (5.571 Debye) has a relatively high dipole moment value that is the evidence of a molecule's high binding affinity, hydrogen bond formation, and non-binding interactions in drug receptor complex [47,48]. While Bis A, Bis B and Bis C show fewer binding interactions, due to their relatively low dipole moment. Therefore, Bis S and Bis AF show relatively more binding interactions to 2E2R.

3.2. Molecular orbital analysis

Frontier molecular orbitals result carry a significant role to predict the possible required energy for chemical reaction. The HOMO (highest occupied molecular orbital) and the LUMO (lowest unoccupied molecular orbital) are substantial for many chemical reactions [49,50]. Electronic absorption relates to the transition from HOMO to LUMO [51]. Chemical hardness and softness are influenced by the HOMO-LUMO gap's value [52,53]. The extended energy gap of a molecule relates to high chemical stability and low chemical reactivity. A low energy gap is related to low chemical stability and high chemical reactivity because of ease transition of electrons [54]. From Table 2 and Fig. 2, the Bis AF has slightly higher energy gap value (5.551 eV), and the Bis S has slightly lower energy gap value (5.272 eV) than that of the other analogues. Bis AF has chemical hardness and softness value 2.775 eV and 0.180 eV, where the hardness value is highest among all the compounds. On the other hand, Bis S has the lowest chemical hardness (5.272 eV) as well as

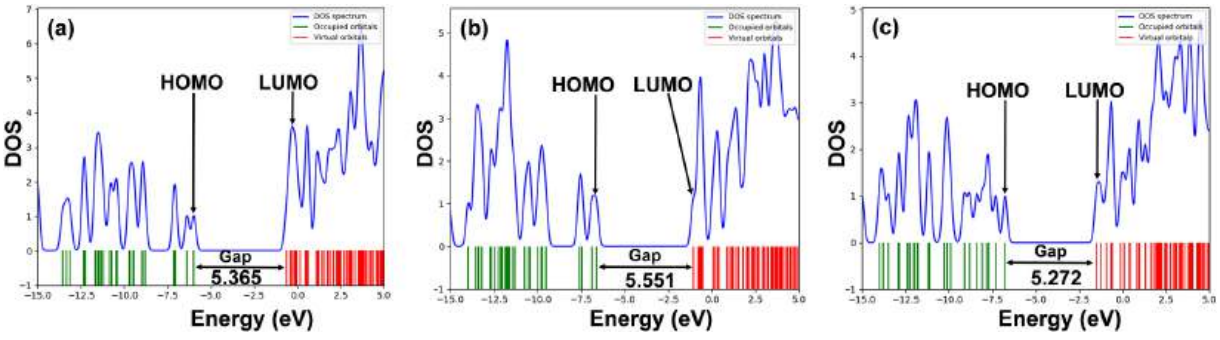

Fig. 2. DOS plot and HOMO-LUMO energy gap of (a) Bis A, (b) Bis AF and (c) Bis S.

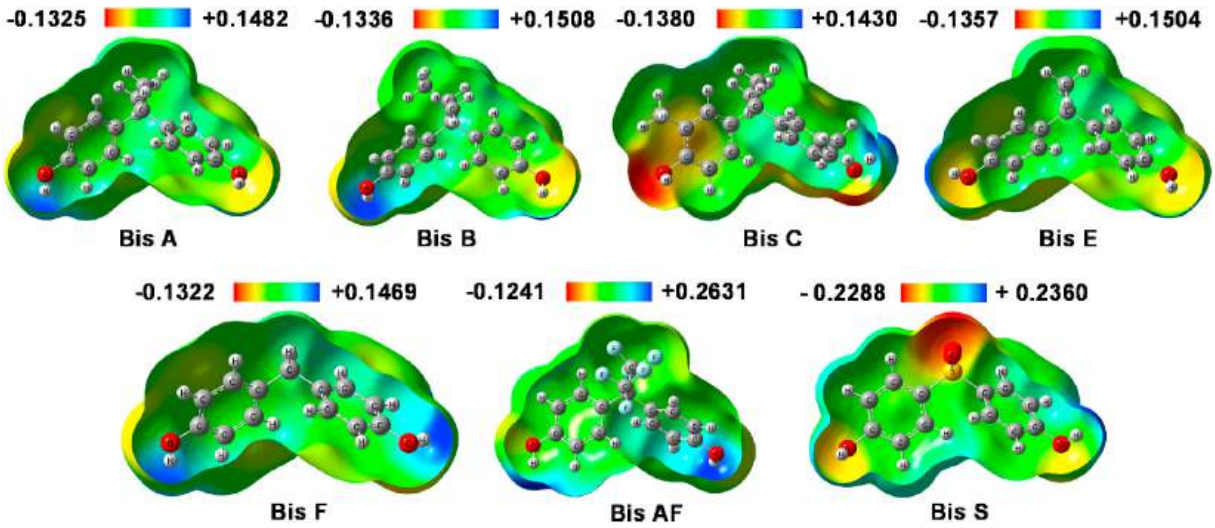

Fig. 3. Molecular electrostatic potential map of bisphenol analogues.

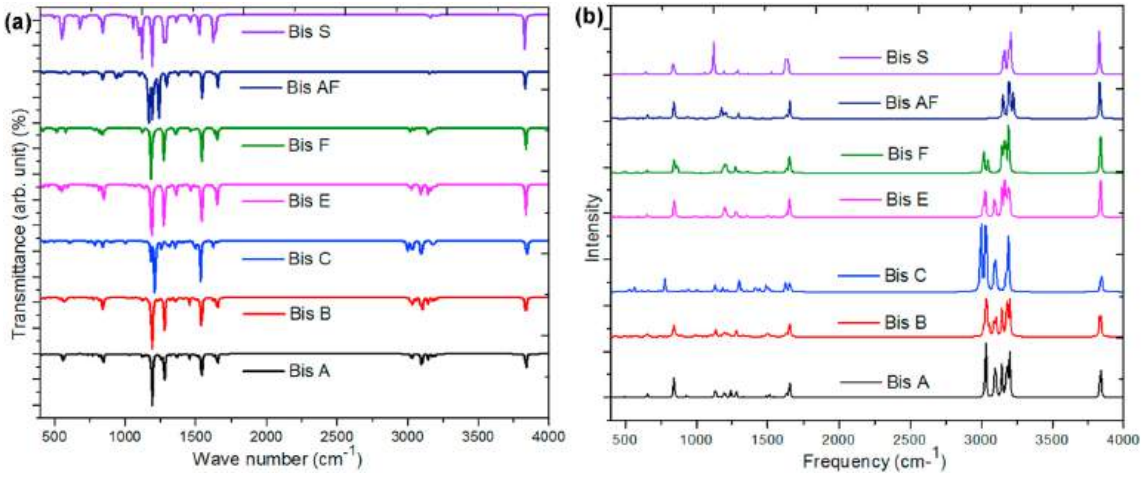

Fig. 4. (a) FT-IR and (b) Raman spectra of bisphenol analogues.

highest chemical softness (0.190 eV). Bis S has SO_2 functional group in the bridging carbon which is the reason behind this high chemical reactivity.

3.3. Molecular electrostatic potential map analysis

Molecular electrostatic potential (MEP) map indicates the total charge of electron and nuclei and give some idea about the nature of electronegativity, partial charge, dipole moment and chemical reactivity of the molecule [55,56]. It represents the possible electrophilic and nucleophilic attack by means of blue and red colors respectively [44]. From MEP map (Fig. 3), maximum negative potentiality has found in oxygen atom and the highest positive potentiality has found for hydrogen atom. Here, Bis S shows the maximum negative potential value (−0.2288 a.u.), meanwhile Bis AF exhibits the highest positive potentiality (+0.2360 a.u.).

3.4. Equilibrium geometry

Because of the presence of different function group at the core structure, it's important to calculate the possible changes in bond lengths and angles to know in details of equilibrium geometry [57]. Results present in Table S1 (atom numbers are indicated in optimized structures Fig. S1). No significant changes in bond lengths, but a very small higher bond angle value was observed in the bridging carbon (C3-C11-C14) of Bis F.

3.5. Vibration frequency and Raman analysis

Vibrational spectroscopy, a combination of FT-IR and Raman spectroscopy known as fingerprint spectroscopic technique, demonstrates unique fingerprint spectra of each molecule by the interaction of electromagnetic radiations in infrared regions (400-4000 cm^{-1}) with the test samples. Both vibrational spectra are highly specific for the identification and structural elucidation of the functional groups in the molecule [58]. The calculated FT-IR vibrational wavenumbers of the Bis analogues have multiplied by the scale factor 0.9679 for the accuracy in their agreement with the experimental data and their tentative vibrational assignments presented (Fig. 4a) [59–61]. The band for O-H stretching vibration in the other analogues exists between 3830 cm^{-1} in Bis S and 3843 cm^{-1} in Bis C, which has shown a significant variance with a small Raman shift from the experimental wavenumbers at 3409.585 and 3372.944 cm^{-1} respectively but supports the established computational calculation (Table S2) [62,63]. The multiple adjacent peaks at 3100-3200 cm^{-1} for C-H stretching around the rings which was found within 3028–3186 cm^{-1} in another study for Bis S [62]. Raman

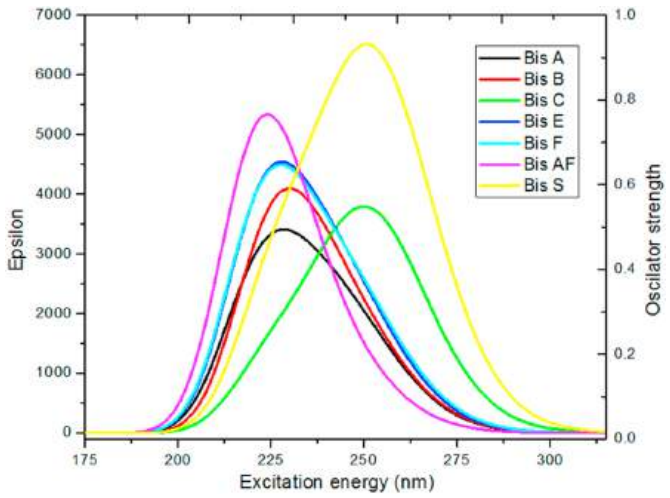

Fig. 5. UV-Visible spectra of bisphenol analogues.

experimental peaks within 3166 cm^{-1} to 3050 cm^{-1} have appointed to 3068 and 3087 cm^{-1} for aromatic C-H stretching [63] and 3000-2850 cm^{-1} aliphatic C-H stretching out of the rings having an agreement with the experimental results (Fig. 4b, Table S2) [64]. In Bis C, a moderate band at 2997 cm^{-1} have observed due to the symmetric stretching of C-H vibrations at the methyl side groups at ortho/meta position of the rings representing a little deviation from other analogues. There has no detectable peak existing in the range of 1700–2900 cm^{-1}. The two sharp peaks for aromatic C-C stretching existed at 1539 and 1652 cm^{-1} are marked out for the experimental peaks at 1510 and 1612 cm^{-1} [65]. The multiple peaks in1539, 1627, 1638, 1652, 1654, and 1655 cm^{-1} are assigned to the Raman experimental peaks 1584 and 1602 cm^{-1} [66]. The dull peaks at 1204, and 1241 cm^{-1} correspond to R1-C-R2 stretching vibration with a mild torsion in the rings [64]. The next bands with low intensities from 1275 to 1292 cm^{-1} have tabulated for C-O stretching with a slight alteration to ~1211 cm^{-1} in Bis C. In Bis S, the S=O stretching vibrations at 1271 and 1119 cm^{-1} show consistency with 1282 and 1139 cm^{-1} for FTIR and Raman vibrational calculation. Any mode of vibration for aliphatic C-C-C stretching has not been seen in compounds except Bis AF where another stretching of C-F bond due to R1-C-R2 vibration was produced at 1239 cm^{-1}. In brief, the highest intensity at ~842 cm^{-1} in the whole experimental spectra corresponds to Raman frequency have attributed to 835, 841, 842, and 843 cm^{-1}. These modes include one or more variations of C–C stretching and scissoring in the rings, C-O stretching and wagging of the attached hydrogen atoms.

The R1-S-R2 stretching vibration calculated at 682 cm^{-1} have assigned at 687 cm^{-1} by the Raman spectrum. These results agree with the experimental molecular orbital analysis of Bis S in which FTIR and Raman frequencies for S-C stretching modes were observed at 690 cm^{-1} and 646 cm^{-1}, respectively [66]. The lower peaks between 555 and 560 cm^{-1} are assigned to the experimental peak at 557 cm^{-1} which represents the twisting of the rings involving C-C-C out-of-plane bending vibrations [62]. The similarity in the assignments occurs for the other three vibrational modes in different combinations of the analogues.

3.6. UV-Vis spectral analysis

The UV-visible spectroscopy using Time-dependent density functional theory (TD-DFT) method is a benchmark for the molecular orbital analysis of fused aromatic ring-system, ensuring the balance between accuracy and computational expense. Each of the two characteristic electronic transition states from the analogues is presented in Table S3 and Fig. 5. In this study, kinetic stability and reactive sites depend on the first electronic transition from the ground state (S_0) to singlet (S_1). Bis S and Bis C show broad absorption bands at 254.10 nm and 252.34 nm along with their oscillator strengths 0.14 and 0.085. Charge transfer of the electron to the excited state $S_0 \rightarrow S_1$ results in the maximum wavelength of the configurations; [(H-4→L), (H→L)] for Bis S and [(H-3→L+4), (H-2→L+5), (H→L)] for Bis C.

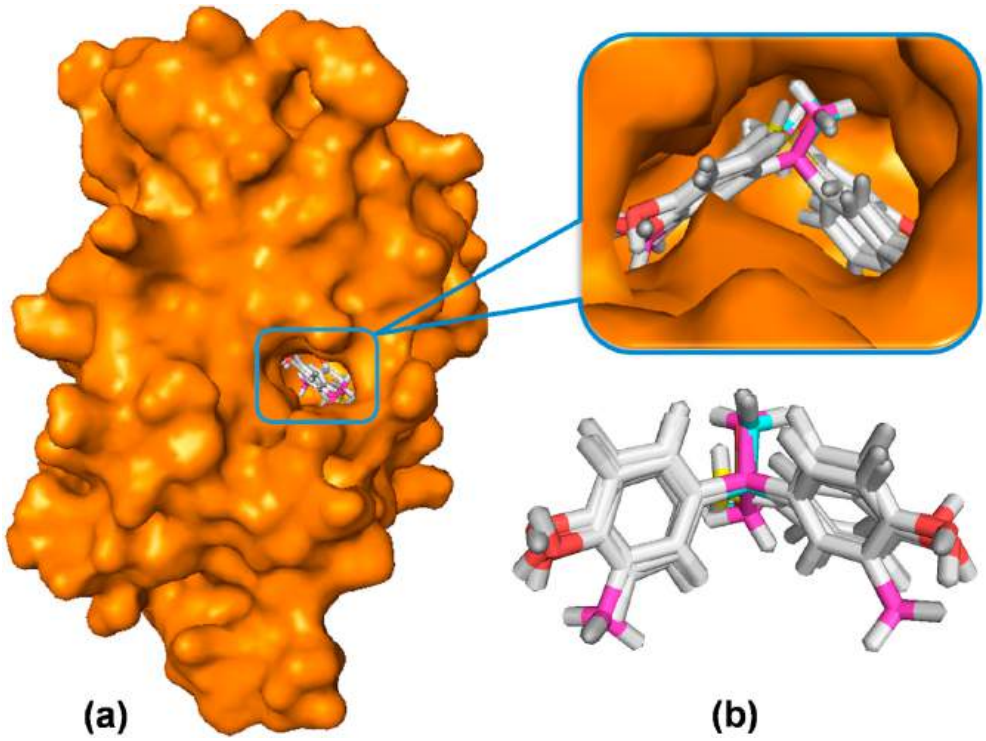

Fig. 6. (a) Docked conformation of bisphenol analogues at inhibition binding site of receptor protein (2E2R), (b) Superimposed view of Bis (A, S, C, F) after docking simulation.

Table 3
Average binding affinity and nonbonding interactions of bisphenol analogues with the receptor protein (2E2R).

Name	Binding affinity (kcal/mol)	Residues in contact	Interaction type	Distance (Å)
Bis A	−8.93	ARG316	PC	4.19395
		ARG316	PC	3.65255
		CYS370	PC	3.99565
		GLU275	Pan	3.87359
		ILE249	PD	2.62099
		PRO246	A	4.09117
		ILE249	A	4.52328
		VAL278	A	4.57943
		PRO246	A	4.11531
		LYS248	PA	5.08491
		ILE249	PA	4.66299
Bis B	−7.67	GLU245	Pan	4.0273
		LYS363	A	5.24348
		TYR315	PA	4.88683
		ARG316	PA	3.83312
		LYS248	PA	5.46922
		ARG316	PA	4.3969
Bis C	−8.07	GLU245	Pan	4.01549
		LYS248	A	4.09495
		LYS363	A	5.11157
		LYS248	A	4.53438
		TYR315	PA	4.88097
		LYS248	PA	5.49904
		ARG316	PA	4.40099
		ARG316	PA	3.90697
Bis E	−9.5	LEU309	PS	2.5889
		MET306	PSu	5.39146
		TYR326	PPS	5.6921
		TYR326	PPTSh	5.26702
		ALA272	A	4.45968
		MET306	A	5.19285
		PHE435	PA	4.2293
		PHE450	PA	5.421
		LEU342	PA	5.22637
		LEU345	PA	5.47238
		ALA431	PA	4.97765
		ALA272	PA	4.89559
		VAL313	PA	5.47073
Bis F	−8.23	ILE249	H	2.36325
		ARG316	PC	3.80934
		GLU275	Pan	4.70324
		ILE249	Pan	4.09848
		LYS248	PA	2.49763
		ILE249	PA	5.11064
		PRO246	PA	4.47379
Bis AF	−9.17	GLU275	H	2.12444
		CYS269	C	2.75346
		LEU268	X	2.97084
		LEU268	X	3.09454
		LEU309	PS	2.68089
		MET306	PSu	5.57372
		TYR326	PPS	5.33854
		TYR326	PPTSh	5.18059
		ALA272	A	4.40779
		ALA272	A	4.30239
		MET306	A	4.70941
		LEU309	A	5.02463
		LEU268	A	4.23416
		PHE435	PA	4.78658
		PHE435	PA	4.77895
		LEU342	PA	5.23909
		ALA431	PA	5.41519
		VAL272	PA	4.78173
		VAL313	PA	5.40919
Bis S	−7.40	GLU275	H	2.22174
		LEU309	PS	2.75394
		MET306	PSu	5.58285
		TYR326	PPS	5.54976
		TYR326	PPTSh	5.15888
		LEU342	PA	5.07996
		ALA431	PA	5.22758
		ALA272	PA	4.74129
		VAL313	PA	5.48252

H = conventional hydrogen bond, A = alkyl, PA = pi-alkyl, PC = Pi-cation, Pa = pi-anion, X = Halogen bond, Pd = Pi-donor, PS = Pi-sigma, PSu = Pi-sulfur, PPS = Pi-Pi stacked, PPTSh = Pi-Pi T-shaped.

Both of the broadband absorption wavelengths at 254.10 nm and 252.34 nm with the highest intensities are mainly due to the electronic transition from HOMO to LUMO. HOMO's electron density focuses C-C double bonds (pi-electrons) in both rings. In contrast, LUMO's electron density is located primarily on the S atom of the S-C bond and the H atom of the O-H bond. The lower energy of excitation corresponding to the HOMO-LUMO energy gap maximizes the chemical reactivity and minimizes kinetic stability [54]. Thus, Bis S and Bis C have more reaction sites, which are confirmed by their low excitation energies, 4.879 and 4.913 eV, respectively.

On the contrary, Bis AF has the least reaction sites with high excitation energy 5.061 eV and tropical oscillator strength 0.022 for the transition $S_0 \rightarrow S_1$. There are three C-F bonds in each of the carbons connected to the bridging carbon between the rings in Bis AF. These bonds reducing their polarizability provide an electrostatic balance in the core making the molecule least reactive. The calculated absorption spectral data of Bis S is in good agreement with its experimental spectra [67]. The other significant excited states exist in Bis A, E and F, having transition energies 5.022, 5.020 and 5.002 eV with a moderate reactive site in their hydroxyl groups.

3.7. Molecular docking and interactions analysis

Electrostatic potential map of receptor protein (Fig. S2) represents the nature of charge and/or potentiality of the protein which may assist to assume the mode of binding mode of ligands. Molecular docking is an important mechanism for hit identification, lead optimization, bioremediation as well as for rational drug design is the interaction of two or more molecules to give the stable adduct. Hereafter, for the establishment of neoteric bioactive substances computer-based biomolecular docking and new lab-based techniques would be the complement each other [68]. However negative values of binding affinity mean the stronger bonding within the receptor protein and Bis analogues (Fig. 6a and b). The non-covalent interactions such as hydrogen bond, halogen bonds as well as hydrophobic interactions are related to the binding of examined structures (Table 3 and Fig. S3). However, strong hydrogen bonding with less than 2.3 Å are subject to dramatically increase the binding affinity [35,69,70]. In docking study, the binding affinity value of Bis E is −9.50 kcal/mol which is highest among all the other derivatives. The binding affinity value of Bis AF (−9.17 kcal/mol) is also high due to strong hydrogen bonds with GLU275 with a distance of 2.12 Å respectively. On the other hand, binding affinity value of Bis B (−7.67 kcal/mol) and Bis S (−7.40 1.08 kcal/mol) are relatively lowest which indicates that these cannot bind properly with receptor protein which means their less estrogenic alteration capacity. Though Bis F contains hydrogen bond, it has relatively low binding affinity value because of larger distance interaction (2.36 Å) than experimental limit (2.30 Å). Moreover, binding affinity or docking score of ubiquitous used analogue Bis C (−8.07 kcal/mol) is less than Bis A (−8.93 kcal/mol) which certify that bond capacity of later one is stronger [71]. The diverse pharmacokinetic parameters (except toxicity) as well as molecular docking support the derivative Bis A than Bis S. Former study found that Bis A forms hydrogen bonds with GLU275 with binding affinity −8.78 kcal/mol [72]. But, the same interaction of Bis AF and Bis S with the

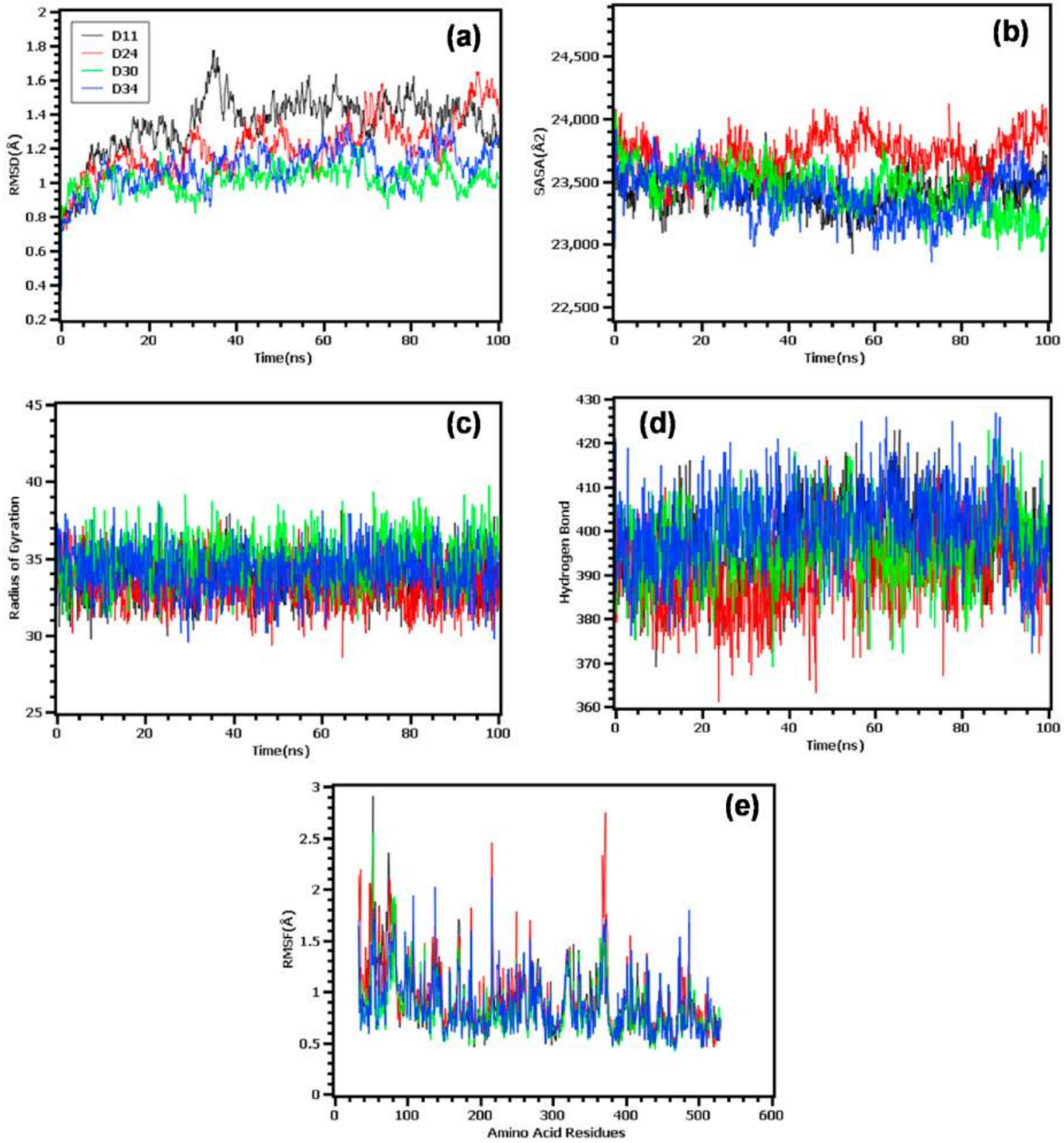

Fig. 7. Result of 100 ns MD simulation of 2E2R in complex with Bis (A, AF, E, AS) ligands (a) RMSD values of docked complexes from C-α atoms. The structural changes of receptor protein by means of (b) SASA, (c) Rg, (d) number of hydrogen bond formed and (e) RMSF respectively.

same residue was found in present investigation. The remaining analogues (Bis A, Bis B, Bis C and Bis F) except Bis E interact with GLU245 with pi-anion bonding instead of hydrogen bond indicating that glutamine, the common residue, interacts with all analogues. Though there is no hydrogen bond in Bis E and conventional hydrogen bonds are found in Bis AF with GLU275 residues only a single carbon hydrogen bond is in Bis AF with CYS269 residue, they play a significant role in binding affinity of Bis E (−9.50 kcal/mol) and Bis AF (−9.17 kcal/mol) which are the highest among the all analogues. Alkyl interactions are found in almost all derivatives with the PRO246, ILE249, VAL278, LYS363, LYS248, ALA272, MET306, LEU309, LEU268 residues respectively.

3.8. Molecular dynamics simulation analysis

The molecular dynamics simulation study of the docked complexes have analyzed to understand the structural variations and stability of the complexes. The Root-Mean Square Deviations (RMSD) of the C-alpha atoms of the complexes have analyzed from the simulation trajectories

Table 4
Pharmacokinetic properties of bisphenol analogues.

Name	Absorption		Distribution		Metabolism		Toxicity					
	HIA	HOB	BBB	P-Gp*I*/P-Gp*S*	CYP3A4*I*/CYP3A4*S*	CYP450 2C9	ERB	ARB	hERG	AOT	Carcinogen	RAT
Bis A	−0.720	−0.600	+0.691	−0.938/-0.932	−0.831/-0.700	NI(0.875)	+0.970	+0.875	WI(0.974)	III	−0.945	1.816
Bis B	+1.000	- 0.643	+0.819	−0.952/-0.918	−0.661/-0.670	I(0.842)	+0.937	+0.870	WI(0.936)	III	−0.563	1.691
Bis C	+0.995	+0.557	+0.801	−0.893/-0.949	−0.827/-0.718	I(0.669)	+0.968	+0.674	WI(0.960)	III	−0.680	1.696
Bis E	+0.995	−0.543	+0.954	−0.954/-0.938	−0.789/-0.797	I(0.679)	+0.891	+0.870	WI(0.951)	II	−0.671	1.719
Bis F	+0.989	−0.614	+0.741	−0.957/-0.971	−0.784/-0.783	NI(0.583)	+0.904	+0.678	WI(0.811)	III	−0.742	1.638
Bis AF	+1.000	- 0.571	+0.924	−0.871/-0.943	−0.721/-0.729	NI(0.611)	+0.897	−0.870	WI(0.934)	III	−0.690	2.026
Bis S	+0.903	+0.514	+0.786	−0.949/-0.991	−0.865/-0.775	I(0.705)	+0.891	+0.870	WI(0.969)	III	+0.566	1.771

HIA=Human Intestinal Absorption, HOB=Human Oral Bioavailability, BBB=Blood-Brain Barrier, P-Gp*I* = P-Glycoprotein Inhibitor, P-Gp*S* = P-Glycoprotein Substrate, CYP3A4*I* = CYP3A4 Inhibition, CYP3A4*S* = CYP3A4 Substrate, ERB = Estrogen Receptor Binding, ARB = Androgen Receptor Binding, hERG = human either a-go-go-gene, AOT = Acute Oral Toxicity, RAT = Rat Acute Toxicity (LD_{50} mol/kg), I=Inhibition, NI= Non-Inhibitor, WI= Weak Inhibitor.

to understand the complexes rigidity. Fig. 7a indicates that, the control as well as the complexes had initial upper rise due to the higher flexibility of the complexes. However, these complexes tend to follow the stable state after 30 ns of time. The complexes Bis AF, and Bis S had higher degree of flexibility compared to the to the complexes which indicates the complexes more flexible nature. However, all complexes had lower RMSD than 2.5 Å at the whole simulations periods which correlates with the complex's stability.

Moreover, the Solvent Accessible Surface Area (SASA) was analyzed to understand the changes in the protein volume where higher SASA related with the expansion of the surface area and the lower SASA defines the truncated nature of the complexes. Fig. 7b indicates that all complexes has similar lower fluctuations in SASA and did not change much volumes of the complexes. The complex Bis E have lower SASA profile than other complexes which correlates with the condensed nature of the complexes. The radius of gyration (Rg) of the complexes has analyzed to understand the mobility of the complexes where the higher Rg defines the higher flexibility. Fig. 7c indicates that the complexes exhibit stable Rg profile across the simulation trajectories.

The hydrogen bond of the systems was also analyzed to find out the stable nature of the complexes, where in Fig. 7d indicate that the complexes have steady hydrogen bonds trend in the simulation. Also, the Root-Mean Square Fluctuations (RMSF) of the complexes have analyzed to understand the flexibility across the amino acid residues of the complexes. Fig. 7e indicates that, almost every residue has lower RMSF than 2.5 Å which defines the complexes stability.

3.9. ADMET analysis

ADMET stands for the absorption, distribution, metabolism excretion and toxicity, the bodies' action on drug which is studied in pharmacokinetics [73]. Hence, it's very important for early drug discovery and development as well as ADMET testing used to investigate all of the properties of a potential drug [74,75]. AdmetSAR represents the Admet score of 18 different properties by value ranging from 0 to 1 where, 0 indicates harmful/toxic and 1 indicates the best. Among the tabulated (Table 4) Admet data HIA (human intestinal absorption), p-glycoprotein inhibitor and substrate, CYP3A4 inhibitor and substrate, hERG (human ether-a-go-go-related gene), acute oral toxicity and carcinogenicity are in listed 18 properties [76]. However, results of AdmetSAR (Table 4) reveal that, most of them also show positive response for HIA except Bis A which denotes that Bis A is the better one because it can be excreted efficiently by urinary and rectal ways comparatively. Bis C and Bis S show positive human oral bioavailability which will able to create health problem while the others are in negative response but all of them are in relatively lower bioavailability value. All the compounds exhibit positive response for the blood-brain barrier, predicting that these compounds will go through BBB which is alarming. All of the derivatives have negative P-glycoprotein inhibition value that means no inhibition to P-glycoprotein and it indicate that they cannot interrupt in the absorption, permeability and retention [77]. The P-glycoprotein substrate usually acts as an inducer or inhibitor according to its functions and it also cause reduction in the bioavailability of the drug if it induced [78]. These bisphenol derivatives show no inhibition to CYP3A4 inhibition and substrate. CYP2C9 is an important cytochrome P450 enzyme where Bis A, Bis F as well as Bis AF show no inhibition. Inhibition causes many of the adverse drug reactions that are associated with the enzyme [79,80]. Estrogen receptor binding and androgen receptor binding are important pharmacokinetic parameters because it can alter the endocrine system and also cause adverse health effect [81]. All the bisphenol derivatives are positive in estrogen receptor and all of them except Bis AF also show positive response in androgen receptor binding which leads to danger health problems. All the bisphenol derivatives except Bis S are non-carcinogenic and all of them have lowest carcinogenic value. All of the derivatives have weak inhibition to human ether-a-go-go-related gene (hERG) which may lead to long QT syndrome, several cardiac side effects and sudden death [82]. Acute toxicity considered as adverse effects which indicates the actions of chemical on human and other living things by different biochemical mechanisms. Acute oral, dermal and inhalation rodent toxicity etc. are important parameters to study about the risk of toxicological effect of chemicals [83]. Moreover, as all of the derivatives exhibit acute oral toxicity in category III, they are comparatively less harmful except Bis E which exhibits acute oral toxicity category II [45]. Here all the bisphenol derivatives LD_{50} values are relatively safe in the range of 1.691–2.026 mol/kg.

4. Conclusion

This investigation reveals the comparative physical, chemical, thermodynamical, spectral, biological and pharmacological analysis of seven most significant bisphenol analogues. Thermodynamic and orbital studies expose their chemical stability and reactivity respectively. Spectral data disclose the comparative characterization of all analogues. Molecular docking, dynamics simulation and nonbonding interactions calculation with the receptor protein (2E2R) express comparative endocrinal effects of bisphenol analogues to the biological system and/or human. ADMET predictions depict their absorption, metabolism, and toxic features. Based on above analysis, this study can be helpful to understand more deeply the biochemical behavior and biological effects of bisphenols, to design alternative candidate and to aware the people about their adverse effects.

Declaration of competing interest

The authors declare that they have no known competing financial interests or personal relationships that could have appeared to influence the work reported in this paper.

Acknowledgement

We are thankful to the department of Chemistry, University of

Chittagong, Bangladesh (www.cu.ac.bd/) for optimization support and Shafi Mahmud, Department of Genetic Engineering and Biotechnology, University of Rajshahi, Bangladesh for MD simulation support.

Appendix A. Supplementary data

Supplementary data to this article can be found online at https://doi.org/10.1016/j.imu.2021.100706.

Author's contribution

MU designed the project, performed all calculation, data collection, and analysis. MU, MKH, SM, AY, SI and AB prepared draft manuscript. MU and MNU revised and finalized the manuscript. All authors read and approve the manuscript.

Funding

This project did not receive any fund.

References

[1] Rochester JR. Bisphenol A and human health: a review of the literature. Reprod Toxicol 2013;42:132–55.
[2] Chen M, Ike M, Fujita M. Acute toxicity, mutagenicity, and estrogenicity of bisphenol-A and other bisphenols. Environ Toxicol An Int J 2002;17:80–6.
[3] Vandenberg LN, Hauser R, Marcus M, Olea N, Welshons WV. Human exposure to bisphenol A (BPA). Reprod Toxicol 2007;24:139–77.
[4] Chen D, Kannan K, Tan H, Zheng Z, Feng Y-L, Wu Y, et al. Bisphenol analogues other than BPA: environmental occurrence, human exposure, and toxicity□ a review. Environ Sci Technol 2016;50:5438–53.
[5] Hongyan L, Zexiong Z, Shiwei X, He X, Yinian Z, Haiyun L, et al. Study on transformation and degradation of bisphenol A by Trametes versicolor laccase and simulation of molecular docking. Chemosphere 2019;224:743–50.
[6] Rosenfeldt EJ, Linden KG. Degradation of endocrine disrupting chemicals bisphenol A, ethinyl estradiol, and estradiol during UV photolysis and advanced oxidation processes. Environ Sci Technol 2004;38:5476–83.
[7] Reddy PVL, Kim K-H, Kavitha B, Kumar V, Raza N, Kalagara S. Photocatalytic degradation of bisphenol A in aqueous media: a review. J Environ Manag 2018;213:189–205.
[8] Geens T, Aerts D, Berthot C, Bourguignon J-P, Goeyens L, Lecomte P, et al. A review of dietary and non-dietary exposure to bisphenol-A. Food Chem Toxicol 2012;50:3725–40.
[9] Gore AC, Chappell VA, Fenton SE, Flaws JA, Nadal A, Prins GS, et al. Executive summary to EDC-2: the Endocrine Society's second scientific statement on endocrine-disrupting chemicals. Endocr Rev 2015;36:593–602.
[10] Giulivo M, de Alda ML, Capri E, Barceló D. Human exposure to endocrine disrupting compounds: their role in reproductive systems, metabolic syndrome and breast cancer. A review. Environ Res 2016;151:251–64.
[11] Richter CA, Birnbaum LS, Farabollini F, Newbold RR, Rubin BS, Talsness CE, et al. In vivo effects of bisphenol A in laboratory rodent studies. Reprod Toxicol 2007;24:199–224.
[12] Vom Saal FS, Akingbemi BT, Belcher SM, Birnbaum LS, Crain DA, Eriksen M, et al. Chapel Hill bisphenol A expert panel consensus statement: integration of mechanisms, effects in animals and potential to impact human health at current levels of exposure. Reprod Toxicol 2007;24:131.
[13] Crain DA, Eriksen M, Iguchi T, Jobling S, Laufer H, LeBlanc GA, et al. An ecological assessment of bisphenol-A: evidence from comparative biology. Reprod Toxicol 2007;24:225–39.
[14] Jalal N, Surendranath AR, Pathak JL, Yu S, Chung CY. Bisphenol A (BPA) the mighty and the mutagenic. Toxicol Reports 2018;5:76–84.
[15] Grumetto L, Barbato F, Russo G. Scrutinizing the interactions between bisphenol analogues and plasma proteins: insights from biomimetic liquid chromatography, molecular docking simulations and in silico predictions. Environ Toxicol Pharmacol 2019;68:148–54.
[16] FDA US. Indirect food additives: Polymers. 2012.
[17] Rosenmai AK, Dybdahl M, Pedersen M, Alice van Vugt-Lussenburg BM, Wedebye EB, Taxvig C, et al. Are structural analogues to bisphenol a safe alternatives? Toxicol Sci 2014;139:35–47.
[18] Russo G, Capuozzo A, Barbato F, Irace C, Santamaria R, Grumetto L. Cytotoxicity of seven bisphenol analogues compared to bisphenol A and relationships with membrane affinity data. Chemosphere 2018;201:432–40.
[19] Cabaton N, Dumont C, Severin I, Perdu E, Zalko D, Cherkaoui-Malki M, et al. Genotoxic and endocrine activities of bis (hydroxyphenyl) methane (bisphenol F) and its derivatives in the HepG2 cell line. Toxicology 2009;255:15–24.
[20] Baradie B, Shoichet MS. Novel fluoro-terpolymers for coatings applications. Macromolecules 2005;38:5560–8.
[21] Matsushima A, Liu X, Okada H, Shimohigashi M, Shimohigashi Y. Bisphenol AF is a full agonist for the estrogen receptor ERα but a highly specific antagonist for ERβ. Environ Health Perspect 2010;118:1267–72.
[22] Viñas P, Campillo N, Martínez-Castillo N, Hernández-Córdoba M. Comparison of two derivatization-based methods for solid-phase microextraction–gas chromatography–mass spectrometric determination of bisphenol A, bisphenol S and biphenol migrated from food cans. Anal Bioanal Chem 2010;397:115–25.
[23] Naderi M, Wong MYL, Gholami F. Developmental exposure of zebrafish (Danio rerio) to bisphenol-S impairs subsequent reproduction potential and hormonal balance in adults. Aquat Toxicol 2014;148:195–203.
[24] Rochester JR, Bolden AL. Bisphenol S and F: a systematic review and comparison of the hormonal activity of bisphenol A substitutes. Environ Health Perspect 2015;123:643–50.
[25] Grignard E, Lapenna S, Bremer S. Weak estrogenic transcriptional activities of Bisphenol A and Bisphenol S. Toxicol Vitro 2012;26:727–31.
[26] Rivas A, Lacroix M, Olea-Serrano F, Laiòs I, Leclercq G, Olea N. Estrogenic effect of a series of bisphenol analogues on gene and protein expression in MCF-7 breast cancer cells. J Steroid Biochem Mol Biol 2002;82:45–53.
[27] Feng Y, Yin J, Jiao Z, Shi J, Li M, Shao B. Bisphenol AF may cause testosterone reduction by directly affecting testis function in adult male rats. Toxicol Lett 2012;211:201–9.
[28] Frisch MJ, Trucks GW, Schlegel HB, Scuseria GE, Robb MA, Cheeseman JR, et al. Gaussian 09, revision A. 02. Gaussian Inc., Wallingford, CT. See Also URL https://www.gaussian.com 2009.
[29] Land H, Humble MS. YASARA: a tool to obtain structural guidance in biocatalytic investigations. Methods Mol Biol 2018;1685:43–67.
[30] Wang J, Wolf RM, Caldwell JW, Kollman PA, Case DA. Development and testing of a general Amber force field. J Comput Chem 2004;25:1157–74.
[31] Harrach MF, Drossel B. Structure and dynamics of TIP3P, TIP4P, and TIP5P water near smooth and atomistic walls of different hydroaffinity. J Chem Phys 2014;140:174501.
[32] Krieger E, Nielsen JE, Spronk CAEM, Vriend G. Fast empirical pKa prediction by Ewald summation. J Mol Graph Model 2006;25:481–6.
[33] Essmann U, Perera L, Berkowitz ML, Darden T, Lee H, Pedersen LG. A smooth particle mesh Ewald method. J Chem Phys 1995;103:8577–93.
[34] Krieger E, Vriend G. New ways to boost molecular dynamics simulations. J Comput Chem 2015;36:996–1007.
[35] Uzzaman M, Hasan MK, Mahmud S, Fatema K, Matin MM. Structure-based design of new diclofenac: physicochemical, spectral, molecular docking, dynamics simulation and ADMET studies. Informatics Med Unlocked 2021:100677.
[36] Uddin Z, Paul A, Rakib A, Sami SA, Mahmud S, Rana S, et al. Chemical profiles and pharmacological properties with in silico studies on elatostema papillosum wedd. Molecules 2021;26.
[37] Mahmud S, Paul GK, Biswas S, Afrose S, Mita MA, Hasan MR, et al. Prospective role of peptide-based antiviral therapy against the main protease of SARS-CoV-2. Front Mol Biosci 2021;8.
[38] Obaidullah AJ, Alanazi MM, Alsaif NA, Albassam H, Almehizia AA, Alqahtani AM, et al. Immunoinformatics-guided design of a multi-epitope vaccine based on the structural proteins of severe acute respiratory syndrome coronavirus 2. RSC Adv 2021;11:18103–21.
[39] Matin MM, Uzzaman M, Chowdhury SA, Bhuiyan MMH. In vitro antimicrobial, physicochemical, pharmacokinetics and molecular docking studies of benzoyl uridine esters against SARS-CoV-2 main protease. J Biomol Struct Dyn 2020:1–13.
[40] Roux MV, Temprado M, Chickos JS, Nagano Y. Critically evaluated thermochemical properties of polycyclic aromatic hydrocarbons. J Phys Chem Ref Data 2008;37:1855–996.
[41] Uzzaman M, Uddin MN. Optimization of structures, biochemical properties of ketorolac and its degradation products based on computational studies. DARU J Pharm Sci 2019;27(1):71–82.
[42] Azam F, Alabdullah NH, Ehmedat HM, Abulifa AR, Taban I, Upadhyayula S. NSAIDs as potential treatment option for preventing amyloid β toxicity in Alzheimer's disease: an investigation by docking, molecular dynamics, and DFT studies. J Biomol Struct Dyn 2018;36:2099–117.
[43] Uddin MN, Uzzaman M, Das S, Al-Amin M, Haque Mijan MN. Stress degradation, structural optimization, molecular docking, ADMET analysis of tiemonium methylsulphate and its degradation products. J Taibah Univ Sci 2020;14:1134–46.
[44] Ramalingam S, Karabacak M, Periandy S, Puviarasan N, Tanuja D. analysis, Gaussian hybrid computational investigation (MEP maps/HOMO and LUMO) on cyclohexanone oximeSpectroscopic (infrared, Raman, UV and NMR). Spectrochim Acta Part A Mol Biomol Spectrosc 2012;96:207–20.
[45] Uzzaman M, Mahmud T. Structural modification of aspirin to design a new potential cyclooxygenase (COX-2) inhibitors. Silico Pharmacol 2020;8:1–14.
[46] Lien EJ, Guo Z, Li R, Su C. Use of dipole moment as a parameter in drug-receptor interaction and quantitative structure-activity relationship studies. J Pharm Sci 1982;71:641–55.
[47] Uzzaman M, Shawon J, Siddique ZA. Molecular docking, dynamics simulation and ADMET prediction of Acetaminophen and its modified derivatives based on quantum calculations. SN Appl Sci 2019;1:1437.
[48] Hoque MJ, Ahsan A, Hossain MB. Molecular docking, pharmacokinetic, and DFT calculation of naproxen and its degradants. Biomed J Sci Tech Res 2018;9:7360–5.
[49] Lewis DFV, Ioannides C, Parke DV. Interaction of a series of nitriles with the alcohol-inducible isoform of P450: computer analysis of structure—activity relationships. Xenobiotica 1994;24:401–8.
[50] Uddin MN, Knock MNH, Uzzaman M, Bhuiyan MMH, Sanaullah AFM, Shumi W, et al. Microwave assisted synthesis, characterization, molecular docking and

pharmacological activities of some new 2′-hydroxychalcone derivatives. J Mol Struct 2020;1206:127678.
[51] Saravanan S, Balachandran V. Quantum chemical studies, natural bond orbital analysis and thermodynamic function of 2, 5-dichlorophenylisocyanate. Spectrochim Acta Part A Mol Biomol Spectrosc 2014;120:351–64.
[52] Parr RG, Zhou Z. Absolute hardness: unifying concept for identifying shells and subshells in nuclei, atoms, molecules, and metallic clusters. Acc Chem Res 1993;26:256–8.
[53] Ayers PW, Parr RG, Pearson RG. Elucidating the hard/soft acid/base principle: a perspective based on half-reactions. J Chem Phys 2006;124:194107.
[54] Aihara J. Reduced HOMO− LUMO gap as an index of kinetic stability for polycyclic aromatic hydrocarbons. J Phys Chem 1999;103:7487–95.
[55] Scrocco E, Tomasi J. The electrostatic molecular potential as a tool for the interpretation of molecular properties. New concepts II. Springer; 1973. p. 95–170.
[56] Matin MM, Hasan S, Uzzaman M, Bhuiyan MH, Kibria SM, Hossain E, et al. Synthesis, spectroscopic characterization, molecular docking, and ADMET studies of mannopyranoside esters as antimicrobial agents. J Mol Struct 2020:128821.
[57] Uddin MN, Siddique ZA, Mase N, Uzzaman M, Shumi W. Oxotitanium (IV) complexes of some bis-unsymmetric Schiff bases: synthesis, structural elucidation and biomedical applications. Appl Organomet Chem 2019;33:e4876.
[58] Billes F, Mohammed-Ziegler I. Vibrational spectroscopy of phenols and phenolic polymers. Theory, Exp. Appl. 2007;42.
[59] Andersson MP, Uvdal P. New scale factors for harmonic vibrational frequencies using the B3LYP density functional method with the triple-ú Basis set 6-311+G(d, p), vol. 2; 2005. p. 2937–41.
[60] Uddin MN, Khandaker S, Amin S, Sumi W, Rahman MA, Rahman SM. Synthesis, characterization, molecular modeling, antioxidant and microbial properties of some titanium (IV) complexes of schiff bases. J Mol Struct 2018;1166:79–90.
[61] Uddin MN, Chowdhury DA, Mase N, Rashid MF, Zaman M, Ahsan A, et al. Spectral and computational chemistry studies for the optimization of geometry of dioxomolybdenum(VI) complexes of some unsymmetrical Schiff bases as antimicrobial agent. J Coord Chem 2018:1–28.
[62] Ullah R, Wang X. Molecular vibrations of bisphenol “S” revealed by FTIR spectroscopy and their correlation with bisphenol “A” disclosed by principal component analysis. Appl Opt 2018;57:D20–6.
[63] Ullah R, Wang X. Raman scattering excited with 532 nm laser in bisphenol “ AF ” and its connection with bisphenol “ A ” and “ S. Spectrosc Lett 2019;52:183–93.
[64] Ullah R, Zheng Y. Raman spectroscopy of “Bisphenol A. J Mol Struct 2016;1108:649–53.
[65] Ullah R, Ahmad I, Zheng Y. Fourier transform infrared spectroscopy of “bisphenol A.”. J Spectrosc 2016;2016:1–5.
[66] Ullah R, Wang X. Raman spectroscopy of Bisphenol ‘S’ and its analogy with Bisphenol ‘A’ uncovered with a dimensionality reduction technique. J Mol Struct 2019;1175:927–34.
[67] Benecyo JE. Scholarly commons @ ouachita simultaneous determination of BPA and BPS using UV/vis spectrophotometry and HPLC. 2016.
[68] Lengauer T, Rarey M. Computational methods for biomolecular docking. Curr Opin Struct Biol 1996;6:402–6.
[69] Matin MM, Bhuiyan MMH, Kabir E, Sanaullah AFM, Rahman MA, Hossain ME, et al. Synthesis, characterization, ADMET, PASS predication, and antimicrobial study of 6-O-lauroyl mannopyranosides. J Mol Struct 2019;1195:189–97.
[70] Uzzaman M, Chowdhury MK, Belal Hossen M. Thermochemical, molecular docking and ADMET studies of aspirin metabolites. Front. Drug, Chem. Clin. Res. 2019;2:1–5.
[71] Moreman J, Lee O, Trznadel M, David A, Kudoh T, Tyler CR. Acute toxicity, teratogenic, and estrogenic effects of bisphenol A and its alternative replacements bisphenol S, bisphenol F, and bisphenol AF in zebrafish embryo-larvae. Environ Sci Technol 2017;51:12796–805.
[72] Babu S, Vellore NA, Kasibotla AV, Dwayne HJ, Stubblefield MA, Uppu RM. Molecular docking of bisphenol A and its nitrated and chlorinated metabolites onto human estrogen-related receptor-gamma. Biochem Biophys Res Commun 2012;426:215–20.
[73] Gill DM, Povinelli APR, Zazeri G, Shamir SA, Mahmoud AM, Wilkinson FL, et al. The modulatory role of sulfated and non-sulfated small molecule heparan sulfate-glycomimetics in endothelial dysfunction: absolute structural clarification, molecular docking and simulated dynamics, SAR analyses and ADMET studies. RSC Med Chem 2021;12:779–90.
[74] Davis AM, Riley RJ. Predictive ADMET studies, the challenges and the opportunities. Curr Opin Chem Biol 2004;8:378–86.
[75] Ferreira LLG, Andricopulo AD. ADMET modeling approaches in drug discovery. Drug Discov Today 2019;24:1157–65.
[76] Guan L, Yang H, Cai Y, Sun L, Di P, Li W, et al. ADMET-score–a comprehensive scoring function for evaluation of chemical drug-likeness. Medchemcomm 2019;10:148–57.
[77] Amin ML. P-glycoprotein inhibition for optimal drug delivery. Drug Target Insights 2013;7:27.
[78] Finch A, Pillans P. P-glycoprotein and its role in drug-drug interactions. Aust Prescr 2014;37:137–9.
[79] Rettie AE, Jones JP. Clinical and toxicological relevance of CYP2C9: drug-drug interactions and pharmacogenetics. Annu Rev Pharmacol Toxicol 2005;45:477–94.
[80] Stubbins MJ, Harries LW, Smith G, Tarbit MH, Wolf CR. Genetic analysis of the human cytochrome P450 CYP2C9 locus. Pharmacogenetics 1996;6:429–39.
[81] Park C, Song H, Choi J, Sim S, Kojima H, Park J, et al. The mixture effects of bisphenol derivatives on estrogen receptor and androgen receptor. Environ Pollut 2020;260:114036.
[82] Lamothe SM, Guo J, Li W, Yang T, Zhang S. The human ether-a-go-go-related gene (hERG) potassium channel represents an unusual target for protease-mediated damage. J Biol Chem 2016;291:20387–401.
[83] Lagunin A, Zakharov A, Filimonov D, Poroikov V. QSAR modelling of rat acute toxicity on the basis of PASS prediction. Mol Inform 2011;30:241–50.